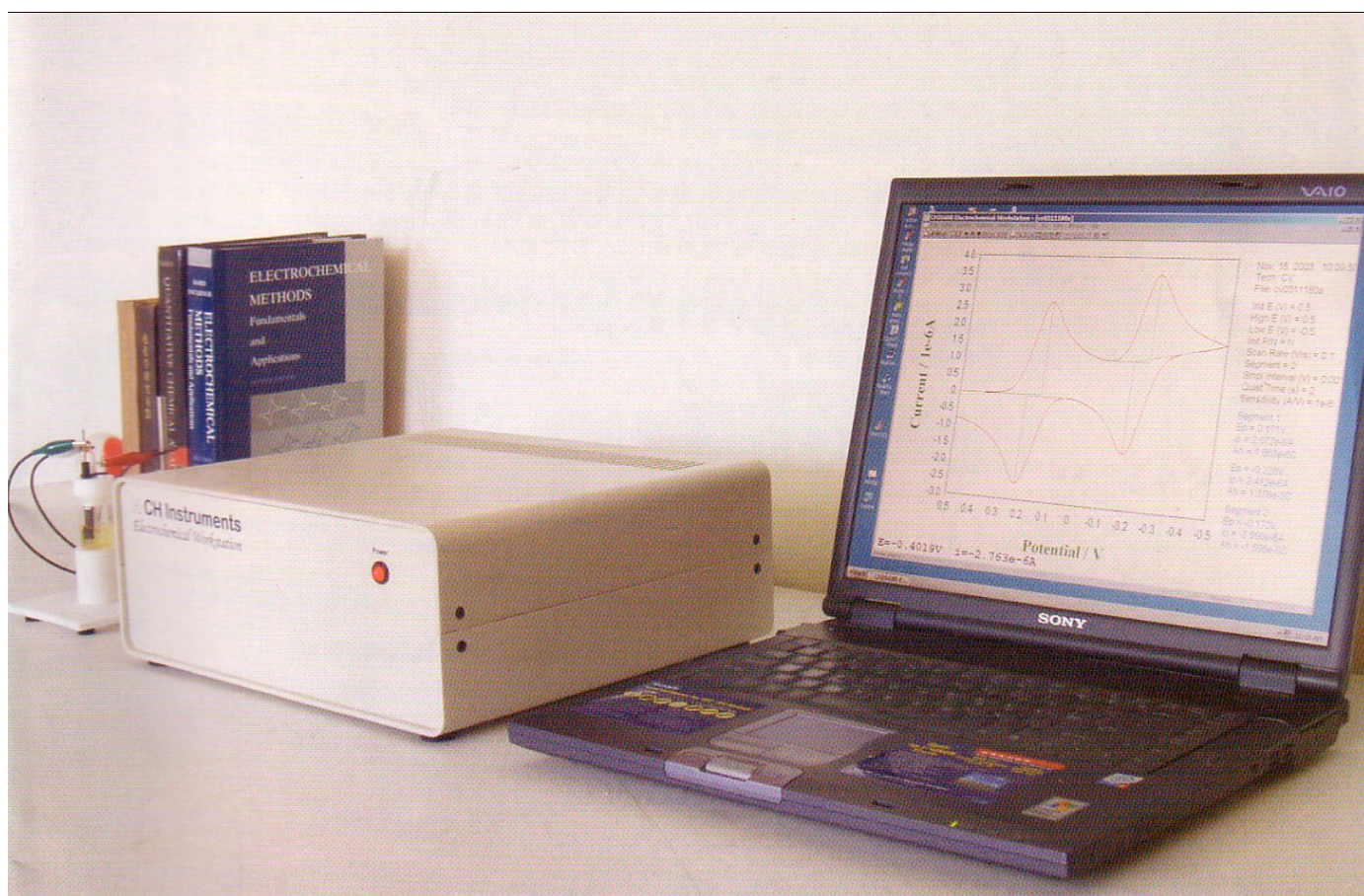


# Scanning Electrochemical Microscope



# Model 900C/910C/920C

## Scanning Electrochemical Microscope

The scanning electrochemical microscope (SECM) was introduced in 1989<sup>1</sup> as an instrument that could examine chemistry at high resolution near interfaces. By detecting reactions that occur at a small electrode (the tip) as it is scanned in close proximity to a surface, the SECM can be employed to obtain chemical reactivity images of surfaces and quantitative measurements of reaction rates. Numerous studies with the SECM have now been reported from a number of laboratories all over the world, and the instrument has been used for a wide range of applications, including studies of corrosion, biological systems (e.g., enzymes, skin, leaves), membranes, and liquid/liquid interfaces.<sup>2</sup> Trapping and electrochemical detection of single molecules with the SECM has also been reported.

The CHI900C/910C/920C Scanning Electrochemical Microscope consists of a digital function generator, a bipotentiostat, high resolution data acquisition circuitry, a three dimensional nanopositioner, and a sample and cell holder. Diagrams for the SECM and cell/sample holder are shown below. The three dimensional nanopositioner has a spatial resolution down to nanometers but it allows a maximum traveling distance of 50 millimeters. The potential control range of the bipotentiostat is  $\pm 10$  V and the current range is  $\pm 250$  mA. The instrument is capable of measuring current down to sub-picoamperes.

In addition to SECM imaging, three other modes of operation are available for scanning probe applications: Surface Patterned Conditioning, Probe Scan Curve, and Probe Approach Curve. Surface Patterned Conditioning allows user to edit a pattern for surface conditioning by controlling the tip at two different potentials and durations. The Probe Scan Curve mode allows the probe to move in the X, Y, or Z direction while the probe and substrate potentials are controlled and currents are measured. The probe can be stopped when the current reaches a specified level. This is particularly useful in searching for an object on the surface and determining approach curves. The Probe Approach Curve mode allows the probe to approach the surface of the substrate. It is also very useful in distinguishing the surface process, using PID control. The step size is automatically adjusted to allow fast surface approach, without letting the probe touching the surface.

The CHI900C is designed for scanning electrochemical microscopy, but many conventional electrochemical techniques are also integrated for convenience, such as CV, LSV, CA, CC, DPV, NPV, SWV, ACV, SHACV, i-t, DPA, DDPA, TPA, SSF, STEP, IMP, IMPE, IMPT, and CP. When it is used as a bipotentiostat, the second channel can be controlled at an independent constant potential, to scan or step at the same potential as the first channel, or to scan with a constant potential difference with the first channel. The second channel works with CV, LSV, CA, DPV, NPV, DNPV, SWV, and i-t.

The CHI900C SECM is an upgrade from the CHI900B SECM. The stepper motor positioner now has a resolution of 4 nanometers with 50 mm travel distance. Since the stepper motor positioner has high enough resolution for most electrochemical scanning probe applications, we will offer the step-motor version SECM. There are two other versions available. The CHI910C will be the stepper motor positioner with a combination of closed loop piezo Z-axis pusher. The CHI920C will be the stepper motor positioner with a combination of closed loop 3-dimensional piezo positioner. The closed-loop piezo control allows improved linearity and reduced hysteresis of the piezo devices.

The other improvements for the CHI900C/910C/920C over the CHI900B/910B include faster data acquisition (1M Hz 16-bit), higher current (250mA), faster CV (1000V/s at 0.1 mV potential increment), and ac impedance measurements.

1. A. J. Bard, F.-R. F. Fan, J. Kwak, and O. Lev, *Anal. Chem.* **61**, 132 (1989); U.S. Patent No. 5,202,004 (April 13, 1993).
2. A. J. Bard, F.-R. Fan, M. V. Mirkin, in *Electroanalytical Chemistry*, A. J. Bard, Ed., Marcel Dekker, New York, 1994, Vol. 18, pp 243-373.

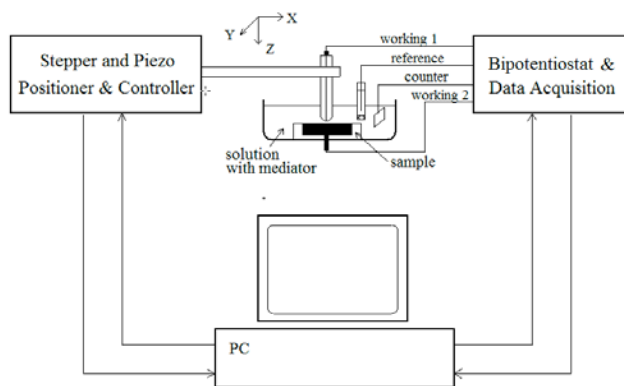
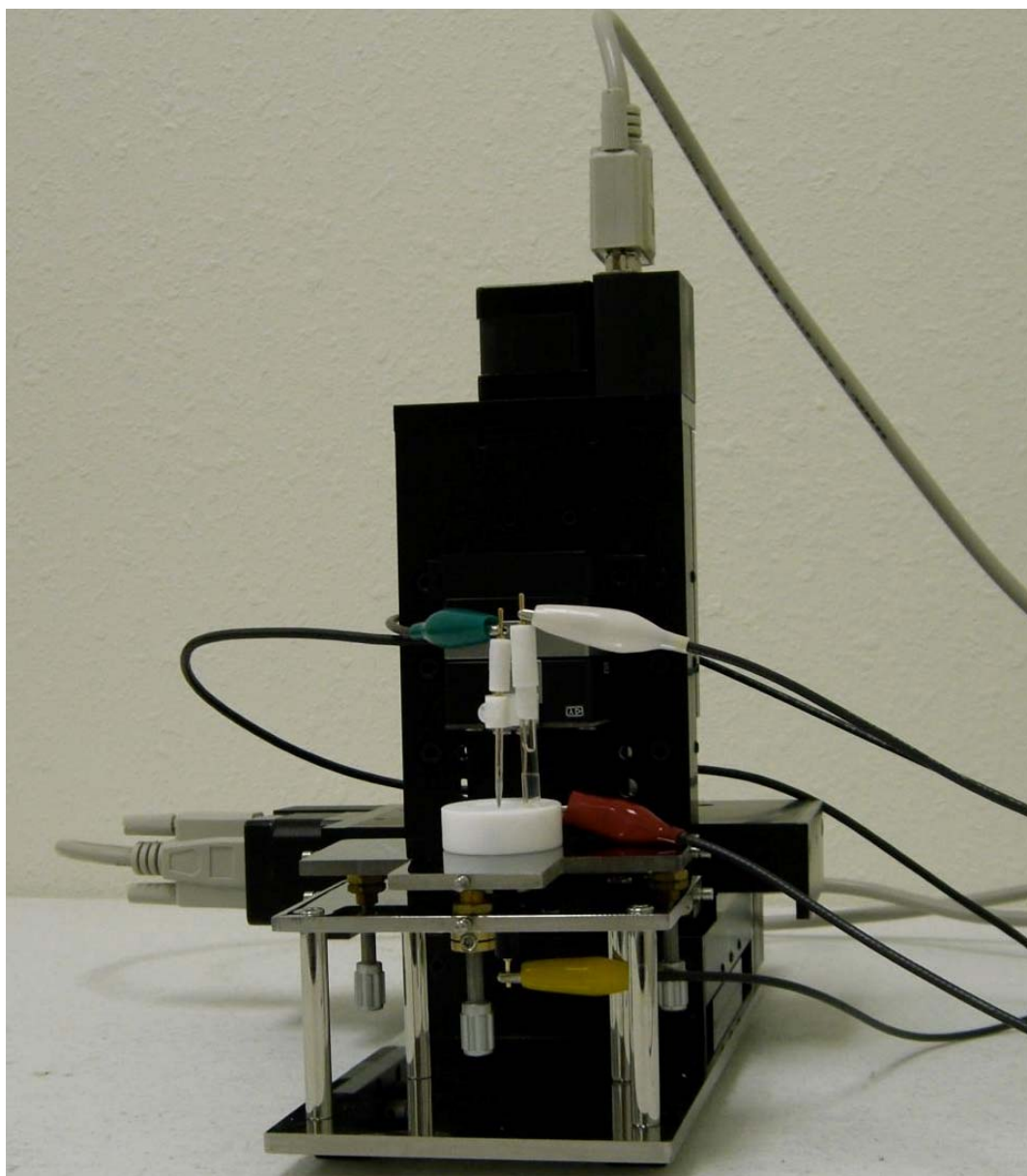
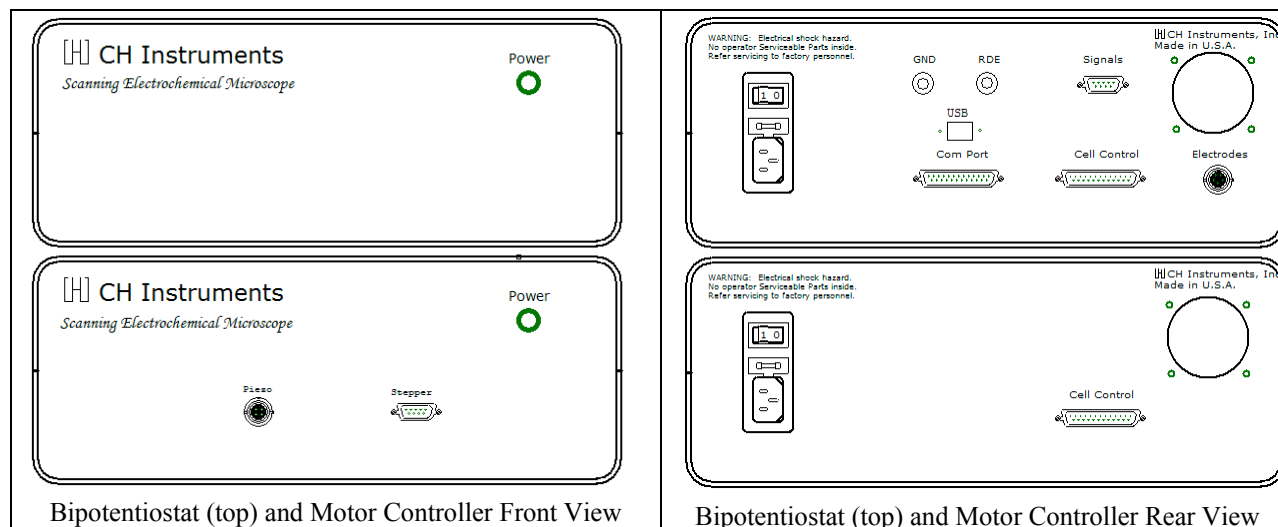


Diagram of Scanning Electrochemical Microscope



Cell/Sample Holder



## CHI900C SECM Specifications

### Nanopositioner:

X, Y, Z resolution: 1.6 nm with Piezo positioner  
4 nm with stepper motor positioner  
X, Y, Z total distance: 5 cm

### Bipotentiostat:

Probe Potential:  $\pm 10$  V  
Substrate Potential:  $\pm 10$  V  
Compliance Voltage:  $\pm 12$  V  
3- or 4-electrode configuration  
Reference electrode input impedance:  $1e12$  ohm  
Current Sensitivity:  $10^{-12}$  A/V to  $10^{-1}$  A/V  
Maximum Current:  $\pm 250$  mA  
External signal recording channel  
ADC Resolution: 16-bit @ 1 M Hz

### Galvanostat:

Current range:  $\pm 250$  mA

### Experimental Parameters:

CV and LSV scan rate: 0.000001 to 10,000 V/s  
Potential increment during scan: 0.1 mV @1000 V/s  
CC and CA pulse width: 0.0001 to 1000 sec  
True integrator for CC  
DPV and NPV pulse width: 0.0001 to 10 sec  
SWV frequency: 1 to 100 kHz  
ACV frequency: 0.1 to 10 kHz  
SHACV frequency: 0.1 to 5 kHz  
IMP frequency: 0.00001 to 100 kHz  
Automatic potential and current zeroing  
Automatic and manual iR compensation  
Current low-pass filters, covering 8-decade frequency range, Automatic and manual setting  
RDE control output: 0-10 V (corresponding to 0-10000 rpm)  
Flash memory for quick software update

## Techniques

### Scanning Probe Techniques

- SECM Imaging (SECM) : constant height, constant current, potentiometric modes
- Probe Approach Curves (PAC)
- Probe Scan Curve (PSC) : amperometric, potentiometric and constant current modes
- Surface Patterned Conditioning (SPC)

### Sweep Techniques

- Cyclic Voltammetry (CV)
- Linear Sweep Voltammetry (LSV)
- Tafel Plot (TAFEL)

### Step and Pulse Techniques

- Staircase Voltammetry (SCV)
- Chronoamperometry (CA)
- Chronocoulometry (CC)
- Differential Pulse Voltammetry (DPV)
- Normal Pulse Voltammetry (NPV)
- Differential Normal Pulse Voltammetry (DNPV)
- Square Wave Voltammetry (SWV)

### AC Techniques

- AC Voltammetry (ACV)
- Second Harmonic AC Voltammetry (SHACV)
- AC Impedance (IMP)
- Impedance versus Potential (IMPE)
- Impedance versus Time (IMPT)

### Galvanostatic Techniques

- Chronopotentiometry (CP)
- Chronopotentiometry with Current Ramp (CPCR)

Serial port or USB port selectable for data communication

**Other Features:**

Real Time Absolute and Relative Distance Display

Real Time Probe and Substrate Current Display

Dual channel measurements for CV, LSV, CA, DPV, NPV, SWV, i-t

Cell control: purge, stir, knock

Automatic potential and current zeroing

Current low-pass filters, covering 8-decade frequency range, Automatic and manual setting

RDE control output: 0-10 V (corresponding to 0-10000 rpm)

Flash memory for quick software update

Serial port or USB port selectable for data communication

Digital CV simulator, user defined mechanisms

Impedance simulator and fitting program

- Multi-Current Steps (ISTEP)
- Potentiometric Stripping Analysis (PSA)

**Other Techniques**

- Amperometric i-t Curve (i-t)
- Differential Pulse Amperometry (DPA)
- Double Differential Pulse Amperometry (DDPA)
- Triple Pulse Amperometry (TPA)
- Integrated Pulse Amperometric Detection (IPAD)
- Bulk Electrolysis with Coulometry (BE)
- Hydrodynamic Modulation Voltammetry (HMV)
- Sweep-Step Functions (SSF)
- Multi-Potential Steps (STEP)
- Electrochemical Noise Measurements (ECN)
- Open Circuit Potential - Time (OCPT)
- Various Stripping Voltammetry
- Potentiometry

**Applications**

- Electrode surface studies
- Corrosion
- Biological samples
- Solid dissolution
- Liquid/liquid interfaces
- Membranes

# Principles and Applications of SECM

## I. Operational Principles of SECM

As in other types of scanning probe microscopes, SECM is based on the movement of a very small electrode (the tip) near the surface of a conductive or insulating substrate.<sup>1</sup> In amperometric SECM experiments, the tip is usually a conventional ultramicroelectrode (UME) fabricated as a conductive disk of metal or carbon in an insulating sheath of glass or polymer. Potentiometric SECM experiments with ion-selective tips are also possible.<sup>2</sup>

In amperometric experiments, the tip current is perturbed by the presence of the substrate. When the tip is far (i.e. greater than several tip diameters) from the substrate, as shown in Fig. 1A, the steady-state current,  $i_{T,\infty}$ , is given by

$$i_{T,\infty} = 4nFDc_a$$

where  $F$  is Faraday's constant,  $n$  is the number of electrons transferred in the tip reaction ( $O + ne \rightarrow R$ ),  $D$  is the diffusion coefficient of species  $O$ ,  $C$  is the concentration, and  $a$  is the tip radius. When the tip is moved toward the surface of an insulating substrate, the tip current,  $i_T$ , decreases because the insulating sheath of the tip blocks diffusion of  $O$  to the tip from the bulk solution. The closer the tip gets to the substrate, the smaller  $i_T$  becomes (Fig 1B). On the other hand, with a conductive substrate, species  $R$  can be oxidized back to  $O$ . This produces an additional flux of  $O$  to the tip and hence an increase in  $i_T$  (Fig. 1C). In this case, the smaller the value of  $d$ , the larger  $i_T$  will be, with  $i_T \rightarrow \infty$  as  $d \rightarrow 0$ , assuming the oxidation of  $R$  on the substrate is diffusion-limited. These simple principles form the basis for the feedback mode of SECM operation.

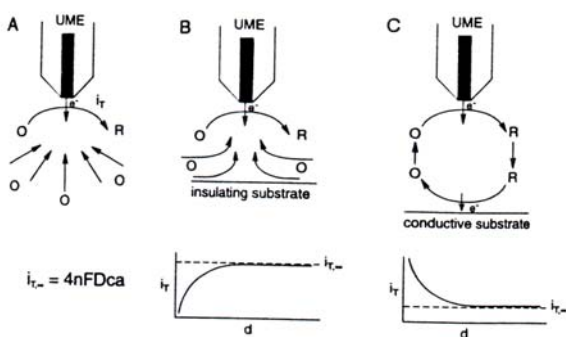


**Figure 1.** Operating principles of SECM. (A). With UME far from the substrate, diffusion of  $O$  leads to a steady-state current,  $i_{T,\infty}$ ; (B). With the UME placed near an insulating substrate, hindered diffusion of  $O$  leads to  $i_T < i_{T,\infty}$ ; (C). with UME near a conductive substrate, positive feedback of  $O$  leads to  $i_T > i_{T,\infty}$ .

When the tip is rastered in the  $x$ - $y$  plane above the substrate, the tip current variation represents changes in topography or conductivity (or reactivity). One can separate topographic effects from conductivity effects by noting that over an insulator  $i_T$  is always less than  $i_{T,\infty}$ , while over a conductor  $i_T$  is always greater than  $i_{T,\infty}$ .

In the feedback mode of the SECM operation as stated above, the overall redox process is essentially confined to the thin layer between the tip and the substrate. In the substrate-generation/tip-collection (SG/TC) mode (when the substrate is a generator and the tip is a collector), the tip travels within a thin diffusion layer generated by the substrate electrode.<sup>1b,3</sup> There are some shortcomings which limit the applicability of the SG/TC mode if the substrate is large: (1). the process at a large substrate is always non-steady state; (2). a large substrate current may cause significant  $iR$ -drop; and (3). the collection efficiency, i.e., the ratio of the tip current to the substrate current, is low. The tip-generation/substrate-collection (TG/SC) mode is advisable for kinetic measurements, while SG/TC can be used for monitoring enzymatic reactions, corrosion, and other heterogeneous processes at the substrate surface.

## II. Applications

### A. Imaging and positioning

A three-dimensional SECM image is obtained by scanning the tip in the  $x$ - $y$  plane and monitoring the tip

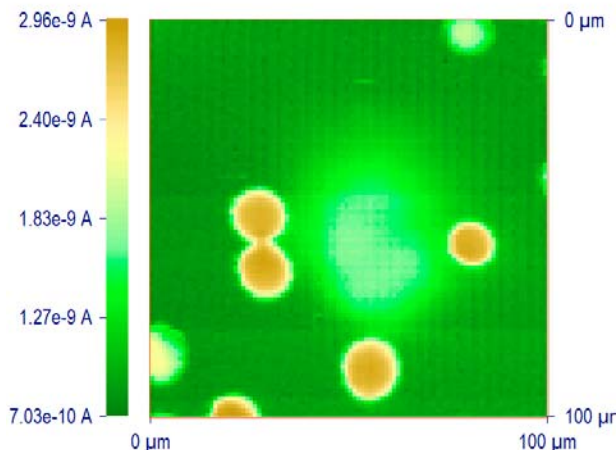


**Figure 2.** SECM image of a polycarbonate filtration membrane with a 2- $\mu$ m-diameter Pt disk UME in  $Fe(CN)_6^{4-}$  solution. Average pore diameter is ca. 10  $\mu$ m.

current,  $i_T$ , as a function of tip location. A particular advantage of SECM in imaging applications, compared to other types of scanning probe microscopy, is that the response observed can be interpreted based on fairly rigorous theory, and hence the measured current can be employed to estimate the tip-substrate distance. Moreover, SECM can be used to image the surfaces of different types of substrates, both conductors and insulators, immersed in solutions. The resolution attainable with SECM depends upon the tip radius. For example, Fig. 2 shows one SECM image of a filtration membrane obtained with a 2- $\mu\text{m}$ -diameter Pt disk tip in  $\text{Fe}(\text{CN})_6^{4-}$  solution. Average pore diameter is ca. 10  $\mu\text{m}$ . An image demonstrating the local activity of an enzymatic reaction on a filtration membrane is shown in Fig. 9 as described below.

### B. Studies of heterogeneous electron transfer reactions

SECM has been employed in heterogeneous kinetic studies on various metal, carbon and semiconductor substrates.<sup>4</sup> In this application, the x-y scanning feature of SECM is usually not used. In this mode, SECM has many features of UME and thin layer electrochemistry with a number of advantages. For example, the characteristic flux to an UME spaced a distance,  $d$ , from a conductive substrate is of the order of  $DC/d$ , independent of the tip radius,  $a$ , when  $d < a$ . Thus, very high fluxes and thus high currents can be obtained. For example, the measurement of the very fast kinetics

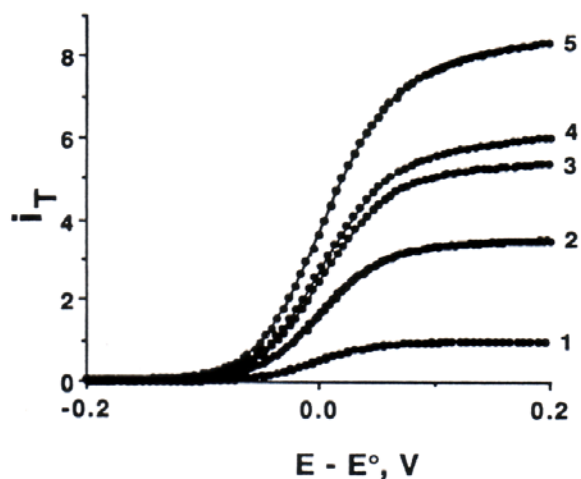


**Figure 3.** Tip steady-state voltammograms for the oxidation of 5.8 mM ferrocene in 0.52 M  $\text{TBABF}_4$  in MeCN at a 1.1- $\mu\text{m}$ -radius Pt tip. Solid lines are theoretical curves and solid circles are experimental data. Tip-substrate separation decreases from 1 to 5 ( $d/a = \infty, 0.27, 0.17, 0.14,$  and  $0.1$ ). (Reprinted with permission from Ref. 4e, copyright 1993, American Chemical Society.)

Of the oxidation of ferrocene at a Pt UME has been carried out.<sup>4e</sup> Five steady-state voltammograms obtained at different distances are shown in Fig. 3, along with the theoretical curves calculated with the values of the kinetic parameters extracted from the quartile potentials. The heterogeneous rate constant,  $k^0$ , obtained ( $3.7 \pm 0.6$  cm/sec) remains constant within the range of experimental error, while the mass-transfer rate increases with a decrease in  $d$ .

### C. Studies of homogeneous chemical reactions

As mentioned above, the TG/SC (with small tip and substrate) mode of SECM, in the same manner as the rotating ring disk electrode (RRDE), is particularly suitable for the studies of homogeneous chemical kinetics.<sup>1b,5</sup> The SECM approach has the advantage that different substrates can be examined easily, i.e., without the need to construct rather difficult to fabricate RRDEs, and higher interelectrode fluxes are available without the need to rotate the electrode or otherwise cause convection in the solution. Moreover, in the TG/SC mode, the collection efficiency in the absence of perturbing homogeneous chemical reaction is near 100%, compared to significantly lower values in practical RRDEs. Finally, although transient SECM measurements are possible, most applications have involved steady-state currents, which are easier to measure and are not perturbed by factors like double-layer charging and also allow for signal averaging. For example, the reductive coupling of both dimethylfumarate (DF) and fumaronitrile (FN) in  $N,N$ -dimethylformamide has been studied with the TG/SC mode.<sup>5a</sup> Fig. 4 shows tip and substrate steady-state voltammograms for the TG/SC regime. Comparable values of both of the plateau currents indicated that the mass

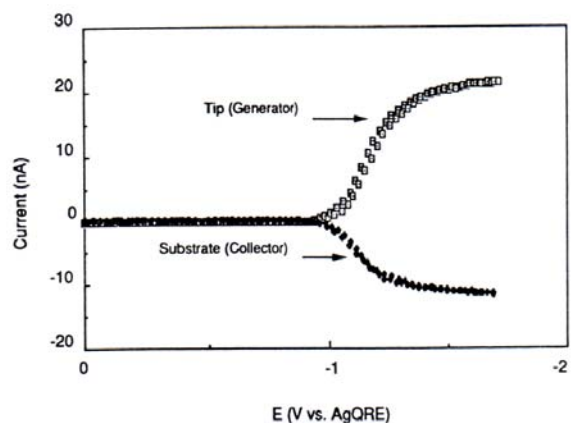


**Figure 4.** SECM voltammograms for FN (28.2 mM) reduction in TG/SC mode.  $d = 1.8$   $\mu\text{m}$ .  $E_T$  was scanned at 100 mV/sec with  $E_S = 0.0$  V vs AgQRE. (Reprinted with permission from Ref. 5a, copyright 1992, American Chemical Society.)

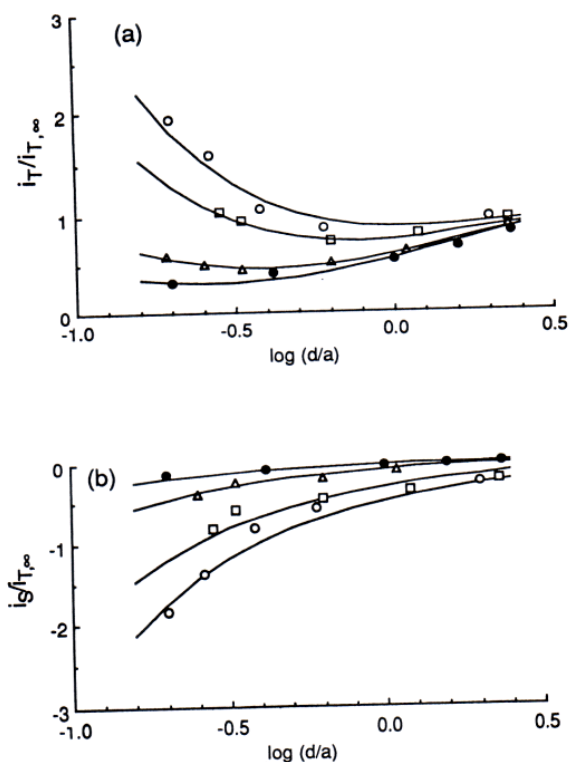


**Figure 5.** Normalized tip (generation, A) and substrate (collection, B) current-distance behavior for FN reduction. FN concentration: (open circle) 1.50 mM, (open square) 4.12 mM, (open triangle) 28.2 mM, and (filled circle) 121 mM.  $a = 5 \mu\text{m}$ , substrate radius is  $50 \mu\text{m}$ . The solid lines represent the best theoretical fit for each set of data. (Reprinted with permission from Ref. 5a, copyright 1992, American Chemical Society.)

transfer rate was sufficiently fast to study the rapid homogeneous reaction. From the approach curves of both tip and substrate currents (Fig. 5) obtained at various FN concentrations, a rate constant  $k_c = 2.0 (\pm 0.4) \times 10^5 \text{ M}^{-1}\text{s}^{-1}$  was determined for the dimerization reactions.

#### D. Characterization of thin films and membranes

SECM is also a useful technique for studying thin films on interfaces. Both mediated and direct electrochemical measurements in thin films or membranes can be carried out. For example, polyelectrolytes, electronically conductive polymers, passivation films on metals and dissolution processes have been investigated by SECM.<sup>6</sup> A unique type of cyclic voltammetry, called tip-substrate cyclic voltammetry (T/S CV), has been used to investigate the

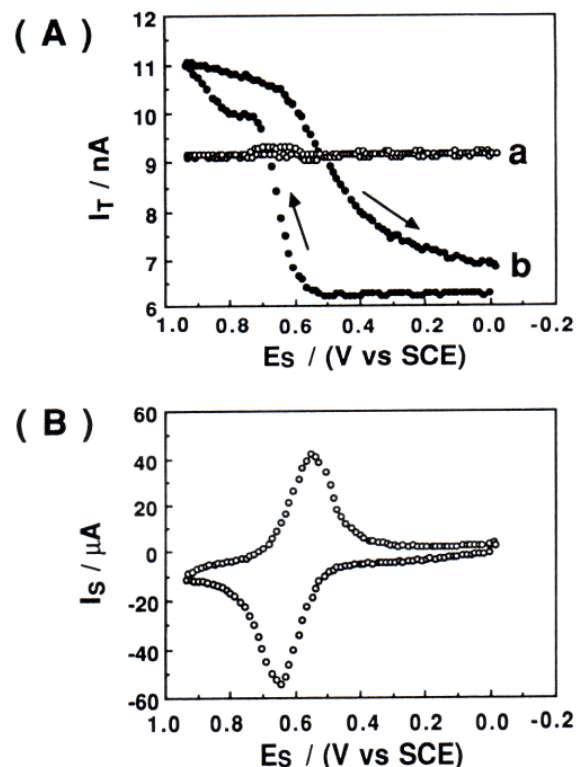


**Figure 6.** T/S CVs (A) curve a,  $d = 500 \mu\text{m}$ , and substrate CV (B) on Nafion/Os(bpy)<sub>3</sub><sup>3+/2+</sup> electrode in  $\text{K}_3\text{Fe}(\text{CN})_6/\text{Na}_2\text{SO}_4$ , scan rate =  $50 \text{ mV/sec}$ ,  $E_T = -0.4 \text{ V vs SCE}$ . (Reprinted with permission from Ref. 6a, copyright 1990, American Chemical Society.)

electrochemical behavior of an Os(bpy)<sub>3</sub><sup>2+</sup>-incorporated Nafion film.<sup>6a</sup> T/S CV involves monitoring the tip current vs. the substrate potential ( $E_S$ ) while the tip potential ( $E_T$ ) is maintained at a given value and the tip is held near the substrate. The substrate CV ( $i_S$  vs.  $E_S$ ) of an Os(bpy)<sub>3</sub><sup>2+</sup>-incorporated Nafion film covering a Pt disk electrode in  $\text{Fe}(\text{CN})_6^{3-}$  solution only shows a wave for the Os(bpy)<sub>3</sub><sup>2+/3+</sup> couple (Fig. 6B), indicating the permselectivity of the Nafion coating. Fig. 6A shows the corresponding T/S CV curves. When the tip is far from the substrate,  $i_T$  is essentially independent of  $E_S$ . When the tip is close to the substrate ( $d = 10 \mu\text{m}$ ), either negative or positive feedback effects are observed, depending on the oxidation state of the Os(bpy)<sub>3</sub><sup>2+/3+</sup> couple in the Nafion. When  $E_S$  is swept positive of the Os(bpy)<sub>3</sub><sup>2+/3+</sup> redox wave, a positive feedback effect is observed due to the regeneration of  $\text{Fe}(\text{CN})_6^{3-}$  in the solution gap region because of the oxidation of  $\text{Fe}(\text{CN})_6^{4-}$  by Os(bpy)<sub>3</sub><sup>3+</sup> at the solution-film interface. When  $E_S$  is negative of the redox wave, the film shows negative feedback behavior, since the



$\text{Os}(\text{bpy})_3^{2+}$  formed is unable to oxidize tip-generated  $\text{Fe}(\text{CN})_6^{4-}$  back to  $\text{Fe}(\text{CN})_6^{3-}$ .

### E. Liquid-liquid interfaces

One of the most promising applications of SECM is the study of charge transport at the interface between two immiscible electrolyte solution (ITIES).<sup>7</sup> Unlike conventional techniques, SECM allows for the studies of both ion and electron transfer at the interface. For example, uphill electron transfer, in which an electron is transferred uphill from a redox couple with a higher standard reduction potential in one phase to another redox couple having a lower standard reduction potential in a second immiscible phase has been demonstrated using the system TCNQ (in 1,2-dichloroethane (DCE))/ferrocyanide (in water).<sup>7c</sup> Fig. 7 shows the approach curve obtained as the UME approaches the interface when the system contains supporting electrolytes with no partitioning ions such as tetraphenylarsonium ( $\text{TPAs}^+$ ). However, the reverse electron flow for the same redox reaction can be induced by employing  $\text{TPAs}^+$  as a potential-determining ion as shown in Fig. 8. The driving force for this reverse electron transfer is the imposition of an interfacial potential difference by the presence in solution of  $\text{TPAs}^+$  in both phases ( $\Delta_o^w\phi = -364$  mV). Note that the detection of reverse electron flow in this case could not be done using the method commonly used for studies of the ITIES, e.g., cyclic voltammetry.

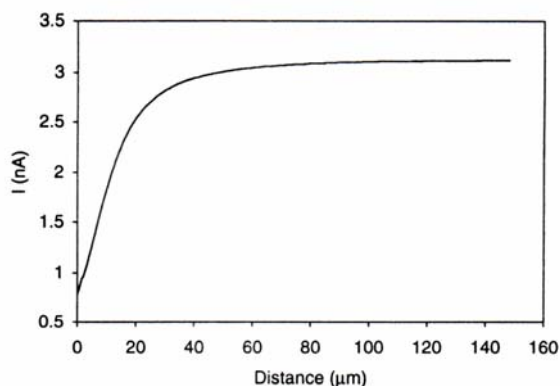


**Figure 7.** Approach curve for the system: 10 mM TCNQ and 1 mM  $\text{TPAsTPB}$  in DCE // 1 mM  $\text{Fe}(\text{CN})_6^{3-}$  and 0.1 M LiCl in  $\text{H}_2\text{O}$ , showing the absence of electron transfer across the liquid/liquid interface. A 25- $\mu\text{m}$ -diameter Pt microelectrode was used to generate  $\text{Fe}(\text{CN})_6^{4-}$  at the electrode tip from the  $\text{Fe}(\text{CN})_6^{3-}$ . Tip potential, -0.4 V vs Ag/AgCl. (Reprinted with permission from Ref. 7c, copyright 1995, American Chemical Society.)

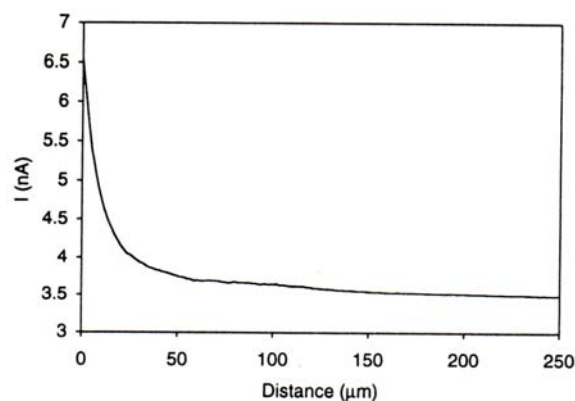


**Figure 8.** Approach curve for the system: 10 mM TCNQ and 1 mM  $\text{TPAsTPB}$  in DCE // 1 mM  $\text{Fe}(\text{CN})_6^{3-}$ , 0.1 M LiCl and 1 mM  $\text{TPAsCl}$  in  $\text{H}_2\text{O}$ , showing reverse electron transfer driven by phase transfer catalyst  $\text{TPAs}^+$ . Tip potential, -0.4 V vs Ag/AgCl. (Reprinted with permission from Ref. 7c, copyright 1995, American Chemical Society.)

Since the ITIES is not polarizable in the presence of  $\text{TPAs}^+$  in both phases, any attempt to impose externally a potential across the interface with electrodes in two phases would result in interfacial ion transfer and a current flow. The SECM approach does not suffer from this interference. Charge transfer processes across the ITIES with or without membranes have also been studied.

### F. Probing patterned biological systems

SECM has been actively employed to probe artificially or naturally patterned biological systems.<sup>8</sup> Both amperometric and potentiometric techniques with ion-selective tips can be used. A direct test of the SECM's ability to image an enzymatic reaction over a localized surface region<sup>8a</sup> is shown in Fig. 9. Glucose oxidase (GO) hydrogel was filled inside small, well-defined pores of polycarbonate filtration membranes. The buffered assay solution contained a high concentration of D-glucose as well as two redox mediators, methyl viologen dication ( $\text{MV}^{2+}$ ) and neutral hydroquinone ( $\text{H}_2\text{Q}$ ). Fig. 9a shows an image obtained with a tip potential of -0.95 V vs. a silver quasi reference electrode (AgQRE) where  $\text{MV}^{2+}$  was reduced to  $\text{MV}^+$ . Since  $\text{MV}^+$  does not react with reduced GO at the hydrogel-filled region, a negative feedback current was obtained. However, with the tip potential changed to 0.82 V, where hydroquinone was oxidized to p-benzoquinone by reduced GO, an increased tip current was observed (Fig. 9b). This positive feedback current over the hydrogel region indicates a significant catalytic feedback of the hydroquinone and provides a direct image of the local enzymatic reaction.

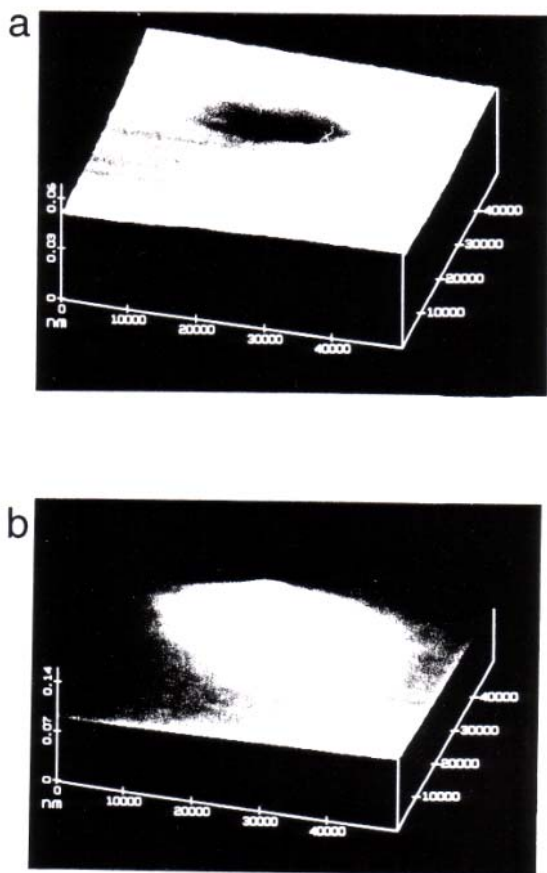


**Figure 9.** SECM images ( $50\ \mu\text{m} \times 50\ \mu\text{m}$ ) of a single GO hydrogel-filled pore on the surface of a treated membrane. Images were taken with a carbon microelectrode tip ( $a = 4.0\ \mu\text{m}$ ). (a). Negative feedback with  $\text{MV}^{2+}$  mediator at tip potential  $-0.95\ \text{V}$  vs AgQRE. (b). Positive feedback with hydroquinone mediator at tip potential  $+0.82\ \text{V}$  vs AgQRE in  $0.1\ \text{M}$  phosphate-perchlorate buffer (pH 7.0) containing  $100\ \text{mM}$  D-glucose,  $50\ \mu\text{M}$  hydroquinone and  $0.1\ \text{mM}$   $\text{MVCl}_2$ . Lightest image regions depict the greatest tip current. (Reprinted with permission from Ref. 8a, copyright 1993, American Chemical Society.)

### G. Fabrication

The SECM can be used to fabricate microstructures on surfaces by deposition of metal or other solids or by etching of the substrate.<sup>9</sup> Two different approaches have been used, the direct mode<sup>9a,b</sup> and the feedback mode<sup>9c</sup>. Typically, in the direct mode, the tip, held in close proximity to the substrate, acts as a working

electrode (in deposition reactions) or as the counterelectrode (in etching processes). The feedback mode of fabrication utilizes the same arrangement as in SECM imaging.

The tip reaction is selected to generate a species that reacts at the substrate to promote the desired reaction, i.e., deposition or etching. For example, a strong oxidant, like  $\text{Br}_2$ , generated at the tip can etch the area of the substrate, e.g., GaAs, directly beneath the tip.<sup>9d</sup> The mediator reactant is chosen to be one that reacts completely and rapidly at the substrate, thus confining the reaction to a small area on the substrate and producing features of area near that of the tip. Small tip size and close tip-substrate spacing are required for high resolution.

### III. References

- (a). A. J. Bard, F.-R. F. Fan, J. Kwak, and O. Lev, *Anal. Chem.* **1989**, *61*, 132; (b). A. J. Bard, F.-R. F. Fan, and M. V. Mirkin in *Electroanalytical Chemistry*, Vol.18 (A. J. Bard, ed.), Marcel Dekker, New York, 1994, p. 243.
- e.g., (a). For a review of early potentiometric SECM experiments, see Ref. 1b; (b). C. Wei, A. J. Bard, G. Nagy, and K. Toth, *Anal. Chem.* **1995**, *67*, 1346; (c). K. Toth, G. Nagy, C. Wei, and A. J. Bard, *Electroanal.* **1995**, *7*, 801; (d). M. Kupper and J. W. Schultze, *Fres. J. Anal. Chem.* **1996**, *356*, 187.
- See also (a). R. C. Engstrom, M. Weber, D. J. Wunder, R. Burgess, and S. Winquist, *Anal. Chem.* **1986**, *58*, 844; (b). R. C. Engstrom, T. Meaney, R. Tople, and R. M. Wightman, *Anal. Chem.* **1987**, *59*, 2005.
- e.g., (a). D. O. Wipf and A. J. Bard, *J. Electrochem. Soc.* **1991**, *138*, 469; (b). B. R. Horrocks, M. V. Mirkin, and A. J. Bard, *J. Phys. Chem.* **1994**, *98*, 9106; (c). R. S. Hutton and D. E. Williams, *Electrochim. Acta*, **1994**, *39*, 701; (d). N. Casillas, P. James, and W. H. Smyrl, *J. Electrochem. Soc.* **1995**, *142*, L16; (e). M. V. Mirkin, T. C. Richards, and A. J. Bard, *J. Phys. Chem.* **1993**, *97*, 7672; (f). M. V. Mirkin, L.O.S. Bulhoes, and A. J. Bard, *J. Am. Chem. Soc.* **1993**, *115*, 201; (g). J. V. Macpherson, M. A. Beeston, and P. R. Unwin, *J. Chem. Soc. Faraday Trans.* **1995**, *91*, 899.
- e.g., (a). F. M. Zhou, P. R. Unwin, and A. J. Bard, *J. Phys. Chem.* **1992**, *96*, 4917; (b). P.R. Unwin and A. J. Bard, *J. Phys. Chem.* **1991**, *95*, 7814; (c). F. M. Zhou and A. J. Bard, *J. Am. Chem. Soc.* **1994**, *116*, 393; (d). D. A. Treichel, M. V. Mirkin, and A. J. Bard, *J. Phys. Chem.* **1994**, *98*, 5751; (e). C. Demaille, P. R. Unwin, and A. J. Bard, *J. Phys. Chem.* **1996**, *100*, 14137.

6. e.g., (a). C. Lee and A. J. Bard, *Anal. Chem.* **1990**, *62*, 1906; (b). C. Lee, J. Kwak, and F. C. Anson, *Anal. Chem.* **1991**, *63*, 1501; (c). J. Kwak, C. Lee, and A. J. Bard, *J. Electrochem. Soc.* **1990**, *137*, 1481; (d). C. Lee and F. C. Anson, *Anal. Chem.* **1992**, *64*, 250. (e). I. C. Jeon and F. C. Anson, *Anal. Chem.* **1992**, *64*, 2021; (f). M. V. Mirkin, F.-R. F. Fan, and A. J. Bard, *Science*, **1992**, *257*, 364. (g). M. Arca, M. V. Mirkin, and A. J. Bard, *J. Phys. Chem.* **1995**, *99*, 5040; (h). M. Pyo and A. J. Bard, *Electrochim. Acta* **1997**, *42*, 3077; (i). E. R. Scott, A. I. Laplaza, H. S. White, and J. B. Phipps, *Pharmaceut. Res.* **1993**, *10*, 1699; (j). S. R. Snyder and H. S. White, *J. Electroanal. Chem.* **1995**, *394*, 177; (k). S. B. Basame and H. S. White, *J. Phys. Chem.* **1995**, *99*, 16430; (l). N. Casillas, S. Charlebois, W. H. Smyrl, and H. S. White, *J. Electrochem. Soc.* **1994**, *141*, 636; (m). D. O. Wipf, *Colloid Surf. A*, **1994**, *93*, 251. (n). E. R. Scott, H. S. White, and J. B. Phipps, *Solid State Ionics* **1992**, *53*, 176; (o). S. Nugnes and G. Denuault, *J. Electroanal. Chem.* **1996**, *408*, 125; (p). M. H. T. Frank and G. Denuault, *J. Electroanal. Chem.* **1993**, *354*, 331; (q). J. V. Macpherson and P. R. Unwin, *J. Chem. Soc. Faraday Trans.* **1993**, *89*, 1883; (r). J. V. Macpherson and P. R. Unwin, *J. Phys. Chem.* **1994**, *98*, 1704; (s). J. V. Macpherson and P. R. Unwin, *J. Phys. Chem.* **1995**, *99*, 14824; **1996**, *100*, 19475; (t). J. V. Macpherson, C. J. Slevin, and P. R. Unwin, *J. Chem. Soc. Faraday Trans.* **1996**, *92*, 3799; (u). K. Borgwarth, C. Ricken, D. G. Ebling, and Heinze, *Ber. Bunsenges. Phys. Chem.* **1995**, *99*, 1421; (v). Y. Y. Zhu and D. E. Williams, *J. Electrochem. Soc.* **1997**, *144*, L43; (w). C. Jehoulet, Y. S. Obeng, Y. T. Kim, F. M. Zhou, and A. J. Bard, *J. Am. Chem. Soc.* **1992**, *114*, 4237; (x). E. R. Scott, H. S. White, and J. B. Phipps, *J. Membrane Sci.* **1991**, *58*, 71; (y). H. Sugimura, T. Uchida, N. Kitamura, and H. Masuhara, *J. Phys. Chem.* **1994**, *98*, 4352; (z). J. E. Vitt and R. C. Engstrom, *Anal. Chem.* **1997**, *69*, 1070.
7. e.g., (a). C. Wei, A. J. Bard, and M. V. Mirkin, *J. Phys. Chem.* **1995**, *99*, 16033; (b). T. Solomon and A. J. Bard, *J. Phys. Chem.* **1995**, *67*, 2787; (c). T. Solomon and A. J. Bard, *J. Phys. Chem.* **1995**, *99*, 17487; (d). Y. Selzer and D. Mandler, *J. Electroanal. Chem.* **1996**, *409*, 15; (e). M. Tsionsky, A. J. Bard, and M. V. Mirkin, *J. Phys. Chem.* **1996**, *100*, 17881; (f). C. J. Slevin, J. A. Umbers, J. H. Atherton, and P. R. Unwin, *J. Chem. Soc. Faraday Trans.* **1996**, *92*, 5177; (g). Y. H. Shao, M. V. Mirkin, and J. F. Rusling, *J. Phys. Chem. B* **1997**, *101*, 3202; (h). M. Tsionsky, A. J. Bard, and M. V. Mirkin, *J. Am. Chem. Soc.* **1997**, *119*, 10785; (i). M.-H. Delville, M. Tsionsky, and A. J. Bard, (submitted to *J. Am. Chem. Soc.* for publication).
8. e.g., (a). D. T. Pierce and A. J. Bard, *Anal. Chem.* **1993**, *65*, 3598; (b). B. R. Horrocks, D. Schmidtke, A. Heller, and A. J. Bard, *Anal. Chem.* **1993**, *65*, 3605; (c). H. Yamada, H. Shiku, T. Matsue, and I. Uchida, *Bioelectrochem. Bioenerg.* **1994**, *33*, 91; (d). B. Grundig, G. Wittstock, U. Rudel, and B. Strehlitz, *J. Electroanal. Chem.* **1995**, *395*, 143; (e). G. Wittstock, K. J. Yu, H. B. Halsall, T. H. Ridgway, and W. R. Heineman, *Anal. Chem.* **1995**, *67*, 3578; (f). H. Shiku, T. Matsue, and I. Uchida, *Anal. Chem.* **1996**, *68*, 1276; (g). J. L. Gilbert, S. M. Smith, and E. P. Lautenschlager, *J. Biomed. Mater. Res.* **1993**, *27*, 1357; (h). C. Kranz, T. Lotzbeyer, H. L. Schmidt, and W. Schuhmann, *Biosens. Bioelectron.* **1997**, *12*, 257; (i). C. Kranz, G. Wittstock, H. Wohlschlager, and W. Schuhmann, *Electrochim. Acta*, **1997**, *42*, 3105; (j). C. Lee, J. Kwak, and A. J. Bard, *Proc. Natl. Acad. Sci. U.S.A.* **1990**, *87*, 1740; (k). R. B. Jackson, M. Tsionsky, Z. G. Cardon, and A. J. Bard, *Plant Physiol.* **1996**, *112*, 354; (l). M. Tsionsky, Z. G. Cardon, A. J. Bard, and R. B. Jackson, *Plant Physiol.* **1997**, *113*, 895.
9. e.g., (a). C. W. Lin, F.-R. F. Fan, and A. J. Bard, *J. Electrochem. Soc.* **1987**, *134*, 1038; (b). D. H. Craston, C. W. Lin, and A. J. Bard, *J. Electrochem. Soc.* **1988**, *135*, 785; (c). D. Mandler and A. J. Bard, *J. Electrochem. Soc.* **1989**, *136*, 3143; (d). D. Mandler and A. J. Bard, *J. Electrochem. Soc.* **1990**, *137*, 2468; (e). O. E. Husser, D. H. Craston, and A. J. Bard, *J. Vac. Sci. Technol. B* **1988**, *6*, 1873; (f). Y.-M. Wu, F.-R. F. Fan, and A. J. Bard, *J. Electrochem. Soc.* **1989**, *136*, 885; (g). H. Sugimura, T. Uchida, N. Shimo, N. Kitamura, and H. Masuhara, *Ultramicroscopy* **1992**, *42*, 468; (h). I. Shohat and D. Mandler, *J. Electrochem. Soc.* **1994**, *141*, 995; (i). S. Meltzer and D. Mandler, *J. Chem. Soc. Faraday Trans.* **1995**, *91*, 1019; (j). C. Kranz, H. E. Gaub, and W. Schuhmann, *Advan. Mater.* **1996**, *8*, 634; (k). J. F. Zhou and D. O. Wipf, *J. Electrochem. Soc.* **1997**, *144*, 1202.

## CHI1550A Picoliter Solution Dispenser

The CHI1550A solution dispenser is designed for making high density and high accuracy solution arrays. Solution arrays are widely used in chemical, biological and medical applications. The solution dispenser consists of a high resolution three dimensional positioner, a piezoelectric jetting device, and a sample platform. The diagram is shown in Figure 1.1.

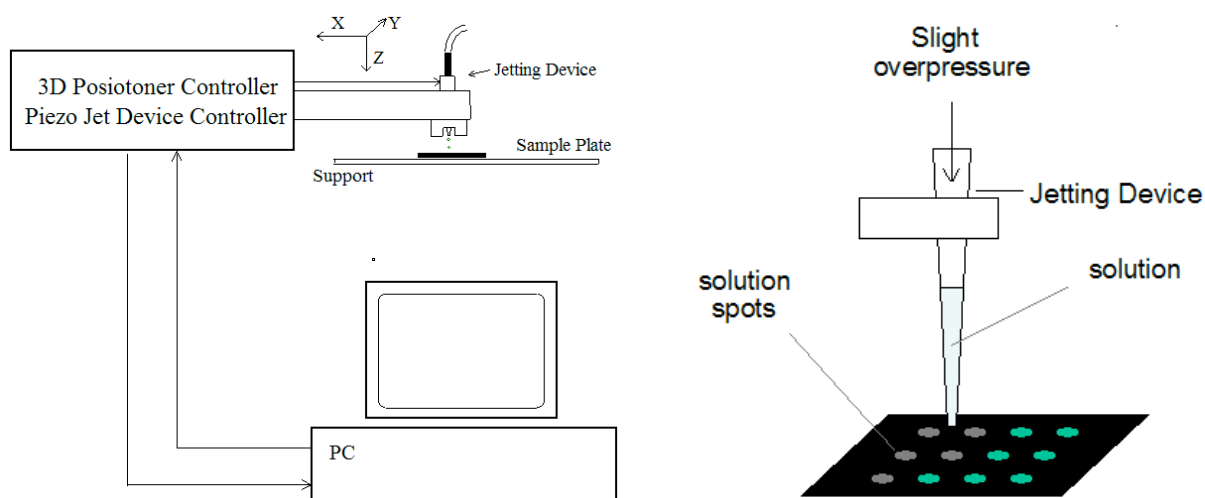


Figure 1. Diagram of the solution dispenser

The three dimensional positioner can travel 50 mm distance for all three axes with 4 nanometer resolution. This allows high precision patterning. This is particularly important when multiple solution components need to be dispensed overlapped.

The jetting device can dispense single drop of fluids. Typical fluids successfully jetted in this device have viscosity less than 40 centipoise and surface tension in the range of 0.02-0.07 N/m. Fluids with properties outside these limits can be jetted if changes to the properties can be achieved with solvents or changes in temperature. With a default 60 micron orifice size, the jetting device can produce drops ranging from 100-200 picoliters in volume depending on the operating parameters and fluids.

The CHI1550A solution dispenser control software is very user-friendly for creating binary, ternary and quadruple arrays of spots containing mixtures of solutions. Instead of using a manually created look-up table for solution dispensing patterns, the software will assist the pattern creation. The software can also provide commonly used patterns as default for binary, ternary and quadruple arrays. The positioner can memorize certain critical positions, such as solution loading point and first dispense point. This will help the jetting device to go to these positions easily and quickly.

The array pattern can be examined graphically. During dispensing process, the array pattern will also be displays as the dispensing progresses.

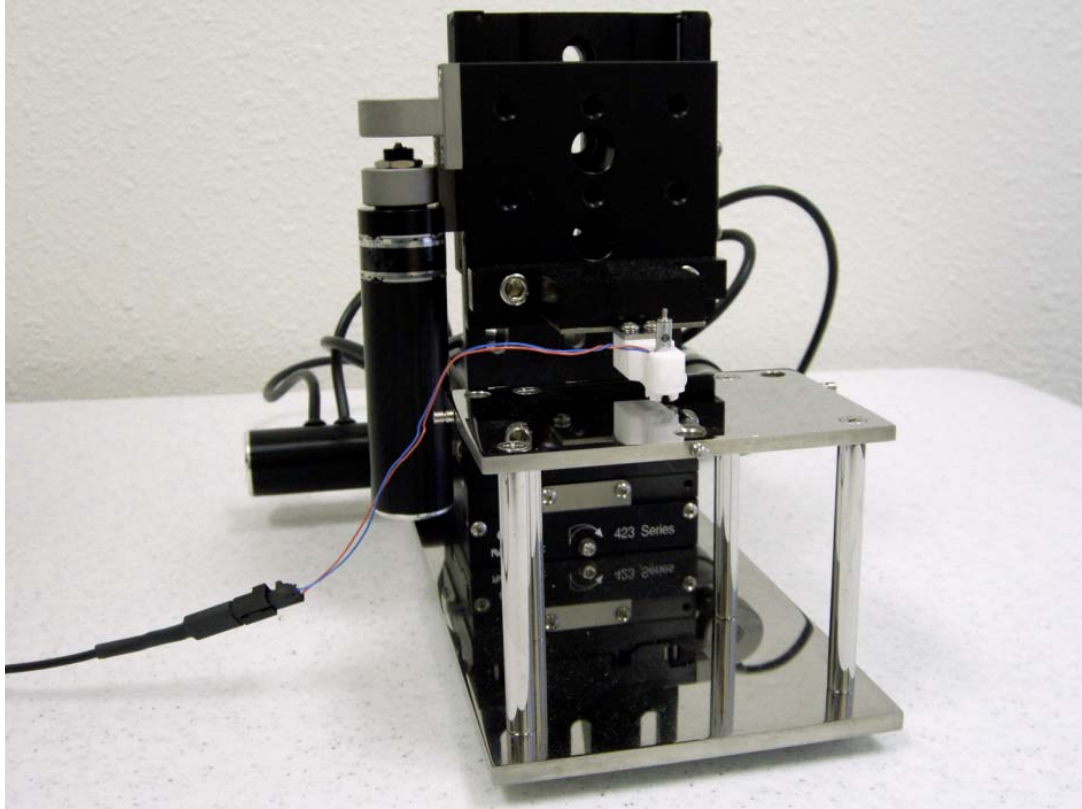


Figure 3. Micropositioner and sample stand

### **System requirements**

*Operating System:* PC with Microsoft Windows 95 / 98 / NT /Me/ 2000 / XP

*Communication:* RS-232 serial port or USB

### **Hardware Specifications**

<b>Micropositioner:</b>	<b>Jetting Device:</b>
Three stepper motors with translation stages <ul style="list-style-type: none"><li>• Maximum range of motion: 50 mm</li><li>• Motor resolution: 4 nm</li><li>• Stall Load: 50 N</li><li>• Maximum Speed: 4 mm / sec</li></ul>	Orifice side of the jetting device: 60 micron Droplet size: 100-200 picoliters Control voltage: 0-150V A protective holder for the jetting device

## Accessories

Part No.	Description	Unit
CHI101	2 mm dia. Gold Working Electrode	1
CHI101P	2 mm dia. Gold Working Electrode	3/pk
CHI102	2 mm dia. Platinum Working Electrode	1
CHI102P	2 mm dia. Platinum Working Electrode	3/pk
CHI103	2 mm dia. Silver Working Electrode	1
CHI104	3 mm dia. Glassy Carbon Working Electrode	1
CHI104P	3 mm dia. Glassy Carbon Working Electrode	3/pk
CHI105	12.5 $\mu\text{m}$ dia. Gold Microelectrode	1
CHI105P	12.5 $\mu\text{m}$ dia. Gold Microelectrode	3/pk
CHI106	25 $\mu\text{m}$ dia. Gold Microelectrode	1
CHI106P	25 $\mu\text{m}$ dia. Gold Microelectrode	3/pk
CHI107	10 $\mu\text{m}$ dia. Platinum Microelectrode	1
CHI107P	10 $\mu\text{m}$ dia. Platinum Microelectrode	3/pk
CHI108	25 $\mu\text{m}$ dia. Platinum Microelectrode	1
CHI108P	25 $\mu\text{m}$ dia. Platinum Microelectrode	3/pk
CHI111	Ag/AgCl Reference Electrode	1
CHI111P	Ag/AgCl Reference Electrode	3/pk
CHI112	Non-Aqueous Ag/Ag <sup>+</sup> Reference Electrode <sup>1</sup>	1
CHI112P	Non-Aqueous Ag/Ag <sup>+</sup> Reference Electrode <sup>1</sup>	3/pk
CHI115	Platinum Wire Counter Electrode	1
CHI116	10 $\mu\text{m}$ dia. Platinum SECM Tip	1
CHI116P	10 $\mu\text{m}$ dia. Platinum SECM Tip	3/pk
CHI117	25 $\mu\text{m}$ dia. Platinum SECM Tip	1
CHI117P	25 $\mu\text{m}$ dia. Platinum SECM Tip	3/pk
CHI118	1-5 $\mu\text{m}$ dia. Platinum SECM Tip	1
CHI120	Electrode Polishing Kit <sup>2</sup>	1

Part No.	Description	Unit
CHI125A	Polished, Bounded, Mounded 100A Ti + 1000 A Gold Crystal for EQCM	1
CHI127	EQCM Cell	1
CHI128	Reference Electrode for EQCM Cell	1
CHI129	Pt Wire Counter Electrode for EQCM Cell	1
CHI130	Thin-Layer Flow Cell	1
CHI131	GC Working Electrode for Flow Cell	1
CHI132	Au Working Electrode for Flow Cell	1
CHI133	Pt Working Electrode for Flow Cell	1
CHI134	Reference Electrode for Flow Cell	1
CHI135	25 $\mu\text{m}$ Spacer for Flow Cell	4/pk
CHI140A	Spectroelectrochemical Cell	1
CHI150	Calomel Reference Electrode	1
CHI151	Mercury/Mercurous Sulfate Reference Electrode	1
CHI152	Alkaline/Mercurous Oxide Reference Electrode	1
CHI172-Model #	Electrode leads for a particular instrument model number	1
CHI200	Picoamp Booster and Faraday Cage <sup>3</sup>	1
CHI201	Picoamp Booster	1
CHI202	Faraday Cage	1
CHI220	Simple Cell Stand <sup>4</sup>	1
CHI221	Cell Top (including Pt wire counter electrode, not a replacement part for the CHI200 cell stand) <sup>5</sup>	1
CHI222	Glass Cell	1
CHI223	Teflon Cap <sup>5</sup>	1
002047	IDA Gold Electrode	1
002048	IDA Platinum Electrode	1
002049	IDA Carbon Electrode	1
011235	CS-2 Remote Controllable Cell Stand	1
011343	QCM Flow Cell	1
TE100	Printed Electrodes (3-electrodes)	40/pk
SE101	3mm dia. Printed carbon electrode	40/pk

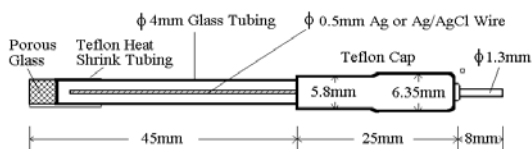
### Notes:

1. A Ag<sup>+</sup> solution (typical 10 mM) should be prepared with the supporting electrolyte and AgNO<sub>3</sub> (not included). This solution is then filled into the reference electrode compartment using a syringe (not included). The instructions will come with the components.
2. The electrode polishing kit contains 1 bottle of 1.0 micron Alpha alumina powder, 1 bottle of 0.3 micron Alpha alumina powder, 3 bottles of 0.05 micron Gamma alumina powder, 2 glass plates for polishing pads, 5 pieces of 73 mm diameter 1200 grit Carbimet disks (grey in color), 5 pieces of 73 mm diameter Mastertex polishing pads (white in color), and 10 pieces of 73 mm diameter Microcloth polishing pads (brown in color).
3. Picoamp Booster and Faraday Cage allows the current measurement down to 1 pA. It is fully automatic and compatible with Model 6xxC and 7xxC series instruments. However, it only works for the primary channel of the 7xxC series.
4. Made of stainless steel and Teflon (see figure below). **Not** remote-controllable. Four glass cells are included.
5. Not a replacement part for the CHI220 Cell Stand.

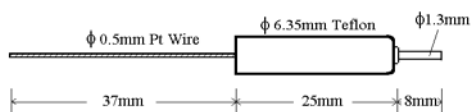
# Accessories and Instrument Chassis



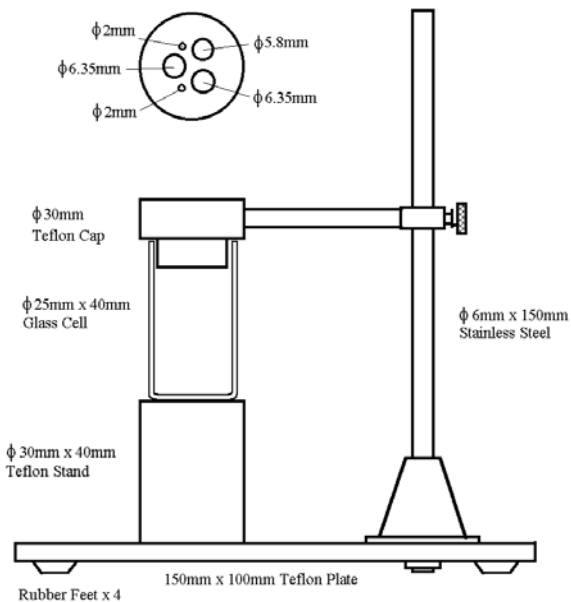
CHI101/102/103/104 Working Electrodes



CHI111/112 Reference Electrodes



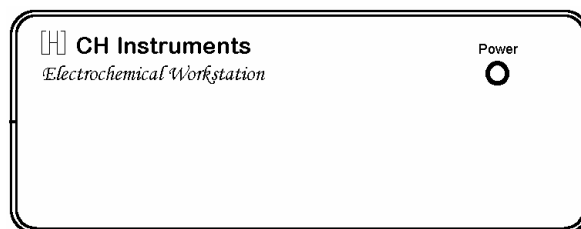
CHI115 Pt Wire Counter Electrode



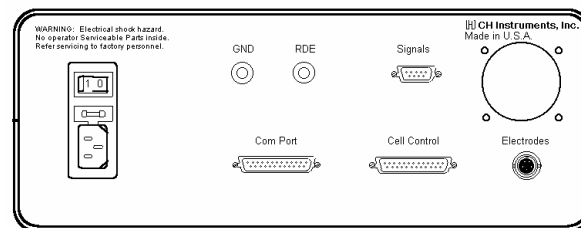
CHI220 Cell Stand



CHI130 Thin-Layer Flow Cell



Front View



Rear View

Front and rear view of the Model 400A, 600B, 700B, 800B, 900B, 1000, and 1100A series instruments



Bridge on Colorado River,  
Austin, Texas



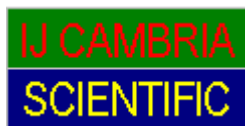
Our office building in  
Austin, Texas.

**Warranty:**

One-year warranty on electronic parts and labour. 90-day warranty on mechanical parts.

**Demo Software:**

Free demo software available upon request.



In Europe

IJ Cambria Scientific .  
11 Gwscwm Road . Burry Port . Carm's . SA16 OBS . UK  
Phone: 01554 835050 . Fax: 01554 835060 . E-mail:  
info@ijcambria.com  
(Mobile: 07957 287343)  
IJ Cambria Scientific: www.ijcambria.com

In US

CH Instruments, Inc.  
3700 Tennison Hill Drive . Austin, TX 78733 . USA